JOURNAL OF CATALYSIS 85, 295–310 (1984)

An EXAFS Study of the Structure of Supported Cobalt Molybdate Catalysts as a Function of Sulfiding Temperature

THOMAS G. PARHAM AND ROBERT P. MERRILL

School of Chemical Engineering, Cornell High Energy Synchrotron Source, Materials Science Center, Ithaca, New York 14852-0294

Received November 23, 1982; revised August 5, 1983

The oxide and sulfide forms of commercially available $CoMo/\gamma\text{-}Al_2O_3$ have been studied with Extended X-ray Absorption Fine Structure (EXAFS). Structural information was obtained for sulfiding temperatures from 25 to 600°C. The oxygen coordination is somewhat uncertain for the oxide form of the catalyst, but values of 3 to 4 are indicated. Neither MoO_3 or $\alpha\text{-}CoMoO_4$ are present. Very mild sulfiding conditions result in formation of Mo–S coordination with no measurable MoS_2, but at increasing sulfiding temperatures, MoS_2 crystallites are formed, their size increasing at the higher temperatures. Crystallite sizes ca. 15 Å are evident between 300 and 400°C. S/Mo ratios of 2 are calculated from EXAFS, considerably lower than implied by total sulfur uptake, with a value of 3, and Mo–S coordination numbers no greater than 4 are observed.

INTRODUCTION

The $CoMo/\gamma\text{-}Al_2O_3$ catalyst system has been studied by a variety of techniques and by many researchers in attempts to determine the structural features of the system and to relate these features to catalytic performance. Little is known concerning the local structure of the Mo or Co on real industrial catalysts and less is known about how this structure changes with preparation method. One reason for this is the difficulty in obtaining useful structural information from X-ray diffraction. Due to the high dispersion of the metals on the alumina support very weak X-ray lines are usually observed, which are not easily deconvoluted from the diffraction patterns of the alumina.

The evidence for the structure of these catalysts has been reviewed by Massoth (*1*), Ratnasamy and Sivasanker (*2*), Furimsky (*3*), and Topsøe (*8*). Pollack *et al.* (*4*) have observed the presence of MoS_2 crystallites on some sulfide catalysts and made estimates of crystallite sizes from line broadening. An EXAFS study of $NiMo/\gamma\text{-}Al_2O_3$ by Kohatsu *et al.* (*5*) has reportedly measured a coordination of 6 sulfur atoms around molybdenum on the sulfide catalyst. More recent studies by Clausen *et al.* (*6, 7*) and by Topsøe *et al.* (*8*) claim that molybdenum is fully sulfided at 400°C and also at milder sulfiding conditions. Mossbauer results suggest that a Co–Mo–S phase may be present on the alumina surface, though no direct evidence of such a phase is present in the EXAFS work.

It is remarkable that a catalyst with such large metal loading (typically 15–20% by weight based on oxides) appears to develop so little crystallinity. As a result the structure of the active commercial catalyst has been, over the years, open to a great deal of speculation with little experimental corroboration. Without the long range ordering which gives rise to X-ray diffraction one would expect that any question relating to the molecular mechanisms cannot be answered without some understanding of the local geometry and coordinations of the catalytically active metals. This kind of situation, i.e., high metal loadings with low degrees of long range order make the system an ideal one for study by Extended X-ray Absorption Fine Structure (EXAFS). EXAFS probes the local order without re-

0021-9517/84 $3.00

course to the existence of long range order and the high loadings mean that there will be minimal interference from the alumina substrate.

One of the difficulties in doing EXAFS on molybdenum has been that most available X-ray sources, even synchrotron sources, decrease seriously in intensity at the *K* absorption edge of Mo (20 keV) and above. With the advent of the Cornell High Energy Synchrotron Source (CHESS) which has very large intensities above 20 keV, it has been possible to conduct EXAFS studies very efficiently in order to determine molybdenum local coordination and structure using EXAFS above the *K* edge.

In this study the reduced, sulfided, and oxide catalysts were examined. Isothermal sulfiding runs were made at temperatures ranging from 25 to 600°C and structural measurements subsequently conducted. Evidence of high dispersion was found in both the oxide and sulfide forms of the catalyst. Marked structural changes were observed upon sulfiding the catalyst. An apparent smooth transition from isolated Mo–S units to small MoS_2 crystallites was observed as sulfiding temperatures were increased.

EXPERIMENTAL METHOD

For this investigation a commercially available $CoMo/\gamma\text{-}Al_2O_3$ catalyst was used. The specifications for this catalyst, American Cyanamid HDS-2A, are given in Table 1 (*9*). All catalyst sulfiding and reducing were carried out in a rotating quartz reactor tube enclosed in a tube furnace. Hydrogen, nitrogen, or a 9:1 mixture of H_2 and H_2S was metered through the reactor at approximately 30 cm^3/min.

Sulfiding was accomplished by exposing a 1-g sample to a nitrogen purge and then to the H_2/H_2S mixture at the selected temperature for 4 h. The reactor was cooled to room temperature under H_2/H_2S flow and then purged with nitrogen for 15 min. It was

TABLE 1

Typical properties American Cyanamid Aero HDS-2A (1)

Composition (wt%)	
Cobalt (CoO)	3.2
Molybdenum (MoO_3)	15.4
Na_2O	0.03
Fe	0.03
Loss on ignition	1.2
Physical properties	
Apparent bulk density (g/cm^3)	0.53
Average diameter (mm)	1.6
Average length (mm)	4.6
Pore volume (cm^3/g)	0.75
Surface area (m^2/g)	310

apparent from work by Massoth and Chung (*1, 10–12*) that this procedure, similar to that used by de Beers *et al.* (*13*) would leave a significant quantity of "nonstoichiometric" sulfur adsorbed on the catalyst at low temperature. This seemed to be an advantage in examining local structure at low sulfiding temperatures where the level of sulfided molybdenum was expected to be small. Temperature treatments were made spanning the range from 25 to 600°C with the expectation of increasing sulfur content with higher temperature. One sample was prereduced with H_2 at 400°C for 2 h prior to sulfiding at 400°C for comparison. A reduced but not sulfided specimen was also prepared.

EXAFS spectra were measured for all prepared catalysts as well as for appropriate model compounds. All EXAFS measurements were in transmission mode. The sulfided and reduced catalysts were protected from air through use of a glovebag and nitrogen purges. Recent measurements have been made *in situ* in a specially designed reactor with results in good agreement with those described above (*14*).

Model compounds included K_2MoO_4, $Na_2MoO_4 \cdot 2H_2O$, MoS_2, $\alpha\text{-}CoMoO_4$, MoO_3, Mo metal foil, and Ba_2CaMoO_6. All measurements were taken at CHESS using a channel-cut Si (220) monochrometer. This monochrometer, combined with the unique

high energy characteristics of CHESS made possible extremely high quality spectra above the Mo K absorption edge (20 keV).

Phase purity of all model compounds was verified by Debye–Scherer and/or diffractometer XRD. Pure α-$CoMoO_4$ was obtained from commercial mixtures of α (olive green) and metastable β (violet) by a combination of shock cooling and physical grinding (*15, 16*).

EXAFS analysis technique. The EXAFS analysis follows that described by Lee *et al.* (*17*) with minor modifications. A single scattering model for the interference in the absorption coefficient may be written as

$$\chi(k) = \frac{\mu - \mu_0}{\mu_0} = -\sum_j \frac{N_j}{kR_j^2} |f_j(k,\pi)| \sin[2kR_j + \delta_j(k)] \cdot \exp(-2\sigma_j^2 k^2) \exp(-2R_j/\lambda_j) \quad (1)$$

where $|f_j(k,\pi)|$ is the backscattering amplitude, $\exp(-2\sigma_j^2k^2)$ is a Debye–Waller correction factor with σ the root mean square displacement of the scattering center, $\exp(-2R_j/\lambda_j)$ is the inelastic scattering loss term with λ representing the inelastic mean free path, $\sin[2kR_j + \delta_j(k)]$ is the sinusoidal interference function with $\delta(k)$ as the scattering phase shift.

The EXAFS transmission spectra were collected as I/I_0 vs E, incident energy. This was converted to μx vs E_0

$$\mu x = -\ln(I/I_0) \quad (2)$$

The selection of the precise threshold energy E_0 is difficult since there is significant structure in the near-edge region. This structure will be discussed in detail for the catalyst in a subsequent paper. In this study E_0 was set at the energy where the absorption coefficient is equal to one-half the edge amplitude. The E_0 adjustment criteria described by Lee, *et al.* (*17*) was used to compensate for any error introduced by our arbitrary initial E_0 selection, and thus to obtain frequency purity in Fourier-filtered features of the interference function.

Once the initial E_0 was specified the data were converted into electron momentum (k):

$$k = \frac{2m(E - E_0)^{1/2}}{h^2} \quad (3)$$

The smoothly varying background ($\mu_0 x$) was then removed by use of a polynomial spline, least squares fit to the data. At this point the data was multiplied by a k^3 weighting factor to compensate for the $1/k$ in Eq. (1) and for the roughly $1/k^2$ behavior of $f|(k,\pi)|$ at large values of k. The desired interference function $\chi(k) \cdot k^3 = (\Delta\mu/\mu_0)k^3$ was obtained by normalizing $(\mu x - \mu_0 x) \cdot k^3$ with respect to $\mu_0 x$. Data sets were generally analyzed over a range of k = 4–16 Å^{-1}.

The interference functions $\chi(k) \cdot k^3$ vs k were Fourier-transformed to provide a qualitative picture of the structural data. The resultant radial structure function is, of course, not a true radial distribution function due to the scattering phase shifts which are convoluted with the phase shifts resulting from interatom propagation. These phase shifts cause the peaks to be shifted approximately 0.4 Å from their correct distances. The amplitudes of peaks in the radial structure function are related to their coordination number, but are also affected by relative backscattering amplitudes and inelastic losses. The radial structure function has been found, however, to be a useful tool for "fingerprinting" the structure of the catalysts. For more precise coordination and distance determinations more complete analysis is required.

By use of Fourier filtering a single set of near neighbors may be isolated from the EXAFS interference function if the peak in the radial structure function is fully resolved. The phase and amplitude functions may then be obtained by inverting the transform of the filtered features. The empirical phase and amplitude functions from known model compounds may be applied to near neighbors of unknown distances with the same absorber–scatterer pair by assuming transferability of phase shift and

amplitude. Much work has been done to verify the validity of these assumptions (*17–20*) with the result that distance calculations may readily be made with an accuracy of ±0.02 Å. Equivalent success may be obtained by use of ab initio calculated phase shift functions. Amplitude transferability is more difficult and less accurate, especially in disordered systems such as that expected on disperse catalysts. Coordination numbers of ±20% can be expected in systems with little disorder.

It is relevant to discuss briefly three phenomena that contribute to the difficulty in calculating accurate coordination numbers. For a more thorough discussion refer to Eisenberger *et al.* (*17, 21, 22*). The first phenomena is thermal disorder due to normal thermal vibration in the lattice. In Eq. (1) this can be accounted for with the Debye–Waller term $\exp(-2\sigma^2k^2)$. A second kind of disorder that may be present especially on a disperse catalyst such as CoMo/γ-Al_2O_3 is configurational disorder. Configurational disorder may be described as local disorder due to numerous different local atomic environments which are phase-averaged in the EXAFS. If the geometric disorder has a Gaussian distribution it is indistinguishable from the Debye–Waller correction unless data are obtained as a function of temperature. When non-Gaussian disorder occurs, the true coordination number is at best difficult to obtain. The peak in the Fourier transform may be broadened, but neither the peak height nor area will be directly proportional to the true coordination number. Much of the important amplitude information is present in the low k portion of the interference function which is, of course, lost due to absorption edge structure which is unavoidably convoluted with the EXAFS interferences. A third phenomena affecting calculation of the coordination is the occurrence of multiple metal–ligand distances in the first shell of near neighbors. This may occur in fully crystalline materials and is not a form of disorder. Nevertheless if the different ligand distances are too similar to produce separately resolved peaks, a complex interference function results along with peak broadening in the radial structure function. In principle the correct individual distances and coordination numbers could be extracted by modeling with sufficient degrees of freedom. Unfortunately it is often true that such modeling does not yield a unique fit to the observed interference function. An example of this type will be discussed later where it occurs in MoO_3, a model compound used in this study.

The real difficulty in determining the coordination in a truly unknown system where disorder is suspected lies in recognizing which of these effects may be responsible for reducing the apparent coordination number. Thermal vibrations can be minimized by cooling specimens, but configurational disorder and multiple first-shell ligand distances cannot be removed. It should be apparent that the use of a Debye–Waller correction in systems such as these may markedly increase error if the latter two effects, which are seldom Gaussian, are also present.

In this study the nearest-neighbor backscattering in model compounds with the absorber–scatterer pairs Mo–O, Mo–S, Mo–Mo were used to calculate the distance and coordination numbers for the oxide, reduced, and sulfided CoMo/γ-Al_2O_3 catalyst. The E_0 adjustment criteria described by Lee *et al.* (*17*) was utilized on single fully resolved coordination shells from the catalysts. E_0 was varied to force the phase difference between the model and unknown phases to pass through the origin, that is $\phi m - \phi u = 0$ at $k = 0$. A nonlinear least squares curve-fitting approach was used to vary R, N, and σ (Debye–Waller factor), with all curve fitting done in k-space. When single shells could not be resolved, doublets were Fourier-filtered and curve-fitted in k-space using variables R, N, σ, and E_0. Of course, in these cases the criteria for E_0 adjustment described above could not be used. In general, however, very good

agreement was obtained between R and ΔE_0 for the two procedures for adjusting E_0.

RESULTS

Model Compounds

Spectra were measured at the Mo K absorption edge (20.002 keV) for the model compounds $Na_2MoO_4 \cdot 2H_2O$, K_2MoO_4, α-$CoMoO_4$, MoO_3, MoS_2, Ba_2CaMoO_6, and Mo metal foil. The Fourier transform for $Na_2MoO_4 \cdot 2H_2O$ is presented in Fig. 1. This radial structure function shows the Fourier transform magnitude in arbitrary units plotted against the distance in Ångstroms from the central Mo atom. A large peak centered at about 1.4 Å represents the four nearest oxygen neighbors at 1.76 Å (*23–25*) which make up the first shell of Mo neighbors. The second shell of neighbors is only barely observable above the noise due to the low backscattering of Na and H_2O and the relatively large distance between Mo atoms.

The interatomic distances for MoO_3, α-$CoMoO_4$, and MoS_2 are included in Table 2 (*26, 15, 27*). MoO_3 is frequently mentioned as one possible chemical form of Mo for the catalyst in oxide form. The radial structure function for MoO_3 is presented in Fig. 2.

TABLE 2

Interatomic Distances for Selected Model Compounds

	Atom pair	Distance, Å (Number)
MoO_3 (18)	Mo–O	1.67 (1)
		1.72 (1)
		1.94 (2)
		2.25 (1)
		2.34 (1)
	Mo–Mo	3.39 (2)
		3.66 (2)
		3.92 (2)
α-$CoMoO_4$ (7, 8)	Mo–O (Type 1)	1.73 (2)
		1.89 (1)
		1.98 (1)
		2.31 (2)
	Mo–O (Type 2)	1.72 (2)
		1.93 (2)
		2.33 (2)
	Mo–Mo	3.34–3.80
	Mo–Co	3.19–3.91
MoS_2(19)	Mo–S	2.41 (6)
	Mo–Mo	3.16 (6)
	Mo–S	3.98 (6)
	Mo–Mo	5.46 (6)
		6.32 (6)
		6.41 (6)

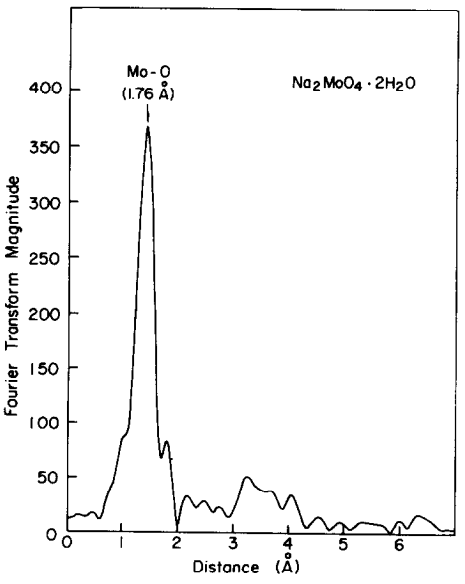

FIG. 1. Fourier transform for $Na_2MoO_4 \cdot 2H_2O$.

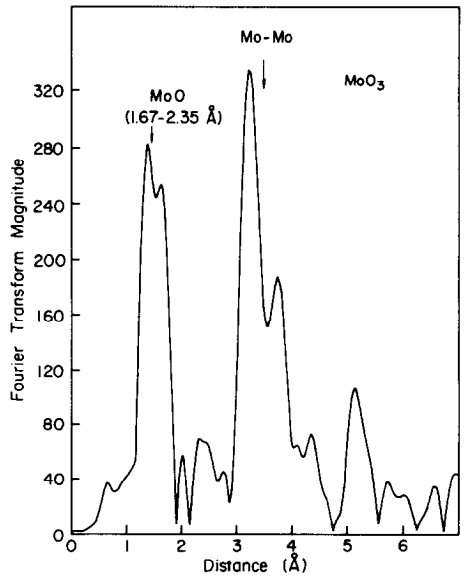

FIG. 2. Fourier transform for MoO_3.

The first peak represents the first set of oxygen neighbors which include five different Mo–O distances ranging from 1.67 to 2.34 Å. The Mo atom is situated in a distorted octahedron in MoO_3, as frequently occurs in Mo compounds. A large peak centered about 3.1 Å represents the second shell of neighbors including six Mo atoms at distances ranging from 3.39 to 3.92 Å. The height of the first peak (Mo–O six-coordinated) is only 280 as compared to the 350 for the four-coordinated Mo–O peak in $Na_2MoO_4 \cdot 2H_2O$ (Fig. 1). The reduction in this height is caused by the interference among the several different Mo–O distances which are too similar to be resolved in the scattering. Calculation of a Mo–O coordination number by area yields a value of 2.6, which is clearly in error. Since the distribution of first-shell distances is not Gaussian, the correct coordination number cannot be obtained by use of a superficial Debye–Waller correction. Use of an empirical amplitude function—in this case from $Na_2MoO_4 \cdot 2H_2O$ as a model compound—to calculate the coordination of MoO_3 is not possible without a modeling approach allowing sufficient degrees of freedom to include all the different distances in the first shell. Such an approach seldom produces a unique structure for such a complicated material and it was not attempted. Similar uncertainties in the coordination number may also be anticipated for the oxide catalyst if Mo on the surface is coordinated in a manner similar to that in bulk MoO_3. Coordination calculations using a single average distance in the least squares fit are included in Table 4. Without Debye–Waller correction, a calculated value of 2.5 is obtained whereas the correct oxygen coordination is known to be 6. If the Debye–Waller correction is made, a calculated coordination of 1.1 is obtained, demonstrating that simple Debye–Waller corrections are not valid in this case, and suggesting that applying such corrections to systems with non-Gaussian disorder can increase the errors in the apparent coordination number. Angle-resolved EXAFS studies on single crystal MoO_3 have been made in order to understand better how to interpret EXAFS of such systems and to obtain more reliable information about local structure. These studies will be reported elsewhere (*28*).

α-$CoMoO_4$ has a complex atomic structure with several different Mo–O distances in the first shell (see Table 2). Fortunately, however, only three different Mo–O distances are sufficiently different to be important to EXAFS. The three Mo–O distances are 1.72 ± 0.01, 1.93 ± 0.04, and 2.32 ± 0.01 Å. All three are separately resolved in the EXAFS spectrum as is apparent in Fig. 3. The doublet at 3.0 Å includes numerous Mo–Mo and Mo–Co distances which are a result of the distorted octahedral coordination of α-$CoMoO_4$.

MoS_2 is of particular interest in this study because of evidence that suggests it may be present on the surface of the active sulfided catalyst. Figure 4 presents the radial structure function for MoS_2. A number of important features should be noted. The peak at 2.0 Å represents the six sulfur neighbors at 2.41 Å. The large peak at 2.8 Å is caused by the six Mo neighbors at 3.16 Å which make

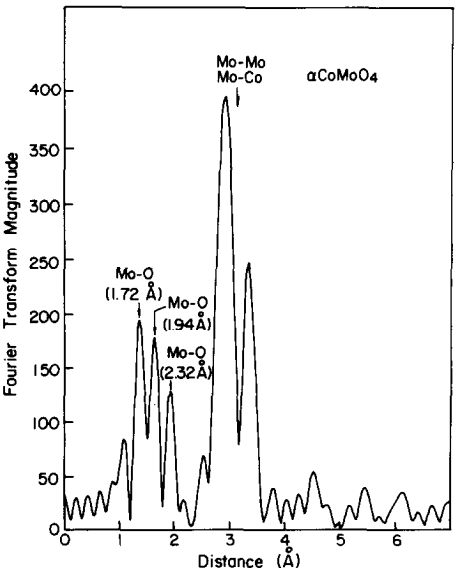

FIG. 3. Fourier transform for α-$CoMoO_4$.

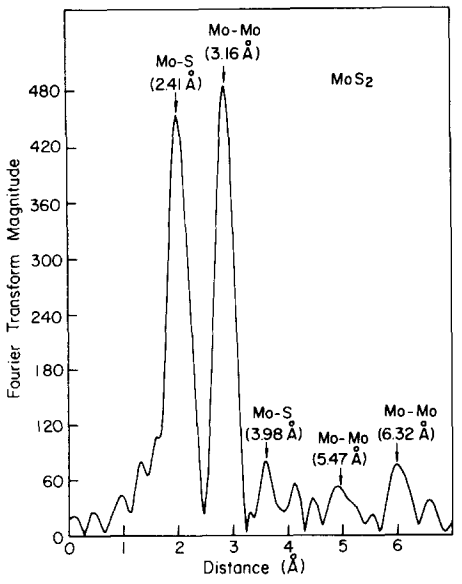

FIG. 4. Fourier transform for MoS_2.

up the first Mo–Mo shell. A small peak at 3.5 Å represents the second Mo–S shell in the basal plane of MoS_2. The reduced magnitude of this peak relative to the first Mo–S shell is a result of the reduced solid angle of outgoing electron flux that is intercepted as well as inelastic losses. The second shell of six Mo–Mo neighbors at 5.46 Å results in a peak at about 5.2 Å and the third shell of six Mo–Mo neighbors at 6.32 results in a peak at about 6.0 Å.

The 6.32-Å third Mo–Mo shell is interesting because of its large amplitude relative to that of the 5.46-Å shell. A single scattering model suggests the outer shell should have 25% lower magnitude than the second Mo–Mo shell. Consideration of inelastic losses would lower this relative value even more. Electron scattering from transition metals, however, is strongly peaked in the forward direction at these energies. In MoS_2 the third Mo–Mo shell is directly aligned with the 3.16-Å first Mo–Mo shell. This alignment allows the forward-scattered electron flux from the first Mo–Mo shell to combine with the primary flux in a "focusing" effect which results in an anomalously high magnitude for the third Mo–Mo shell. Similar multiple scattering effects have been discussed with respect to copper (*29, 30*). This multiple scattering effect is caused by the unique alignment of Mo atoms in MoS_2 and thus provides a feature which is indicative of crystalline MoS_2 on the catalyst.

Three kinds of tests were made of the phase transferability assumption. The first test involved using phase and amplitude functions described by Cramer *et al.* (*19*) to calculate the distances in several model compounds and then comparing these distances to the known interatomic distances. The results of this study are presented in Table 3a. For each "unknown" atom pair examined the calculated interatomic distance R_{calc} is compared to the actual distance R_{act} which is known from XRD. The error between actual and calculated distances is also presented. The agreement between calculated and actual distances is generally within 0.02 Å. As a second test of phase transferability, tabulated phase functions by Teo and Lee (*31*) were used to obtain R_{calc} for all model compounds. In all cases agreement was within 0.02 Å.

The third method used to test phase transferability utilized the Mo–O functions obtained from K_2MoO_4 (*32*) to calculate the Mo–O distances in α-$CoMoO_4$ and $Na_2MoO_4 \cdot 2H_2O$. The Mo–Mo first and second shells in Mo metal were used to calculate other Mo–Mo distances in Mo metal and in MoS_2. The first Mo–S distance in MoS_2 was used to calculate the second Mo–S distance in MoS_2. These results are also

TABLE 3a

Interatomic Distance Comparisons

Bond	Model	Unknown	R_{act} (Å)	R_{calc} (Å)	Error (Å)
Mo–O	Cramer (11)	K_2MoO_4	1.76	1.73	0.03
Mo–O	Cramer (11)	$Na_2MoO_4 \cdot 2H_2O$	1.76	1.74	0.02
Mo–S	Cramer (11)	MoS_2	2.41	2.42	0.01
Mo–S	Cramer (11)	MoS_2	3.98	3.98	0.00
Mo–Mo	Cramer (11)	MoS_2	3.16	3.17	0.01
Mo–Mo	Cramer (11)	Mo	2.73	2.71	0.02
Mo–Mo	Cramer (11)	Mo	3.15	3.16	0.01
Mo–Mo	Cramer (11)	Mo	4.45	4.45	0.00

TABLE 3b

Interatomic Distance Comparisons

Bond	Model	Unknown	R_{act} (Å)	R_{calc} (Å)	Error (Å)
Mo–O	K_2MoO_4	$Na_2MoO_4 \cdot 2H_2O$	1.76	1.77	0.01
Mo–O	$Na_2MoO_4 \cdot 2H_2O$	$\alpha CoMoO_4$	1.73 ± 0.01	1.72[a]	0.01
Mo–O	$Na_2MoO_4 \cdot 2H_2O$	$\alpha CoMoO_4$	1.93 ± 0.04	1.91[a]	0.02
Mo–O	$Na_2MoO_4 \cdot 2H_2O$	$\alpha CoMoO_4$	2.32 ± 0.01	2.35[a]	0.03
Mo–S	MoS_2 (2.41)	MoS_2 (3.98)	3.98	3.99	0.01
Mo–Mo	Mo (3.15)	MoS_2	3.16	3.15	0.01
Mo–Mo	Mo (2.73)	Mo (3.15)	3.15	3.18	0.03
Mo–Mo	Mo (2.73)	Mo (4.45)	4.45	4.46	0.01

[a] Two shell curve fit due to incomplete resolution.

presented in Table 4. Agreement is generally within 0.02 Å, with 0.03 Å the largest error obtained. Consequently, for this work the phase shifts obtained from our own model compounds were used for all calculations.

Two tests were made of the accuracy of coordination numbers calculated with EXAFS. The first test involved application of amplitude and phase functions from Cramer *et al.* (*19, 20*) to model compounds measured in this study. The results are presented in Table 4a. The average error without Debye–Waller correction was 17%, with a maximum error of 28%. With Debye–Waller correction ($N\sigma$ in Table 4a) the average error was 7% and the maximum error was 16%. The second test involved ap-

TABLE 4a

Coordination Comparison with Cramer *et al.* (*19, 20*)

Distance	Model	Unknown	N_{act}	N_{calc}	Error (%)	$N\sigma_{calc}$	Error (%)
Mo–O	Cramer	K_2MoO_4	4	3.7	7	3.8	5
Mo–O	Cramer	$Na_2MoO_4 \cdot 2H_2O$	4	3.1	22	3.8	5
Mo–S	Cramer	MoS_2	6	6.6	10	6.2	3.3
Mo–Mo	Cramer	Mo (2.73)	8	10.2	28	9.3	16

TABLE 4b

Coordination Calculations on Model Compounds

Distance	Model	Unknown	N_{act}	N_{calc}	Error (%)	$N\sigma_{calc}$	Error (%)
Mo–O	$Na_2MoO_4 \cdot 2H_2O$	K_2MoO_4	4	3.4	15	3.7	7.5
Mo–Mo	Mo (3.15)	MoS_2	6	5.8	3	7.1	19
Mo–O	$Na_2MoO_4 \cdot 2H_2O$	MoO_3	6	2.5	58	1.1	82

plication of one measured model compound to another where this was possible. The amplitude functions from the Mo–O first-coordination peak for $Na_2MoO_4 \cdot 2H_2O$ was used to calculate the amplitude of the Mo–O coordination in K_2MoO_4. The second Mo–Mo coordination peak in Mo metal (3.15 Å) was used to calculate the coordination number for the Mo–Mo 3.16 Å peak in MoS_2. The average error in this test was 9% without and 18% with Debye–Waller correction. The maximum errors were 15% without and 19% with Debye–Waller correction. Also included in Table 4b are the results from a single-shell calculation on MoO_3. The very large error in this example illustrates the problems associated with fitting multiple unresolved distances as a single shell. In this case, a two-distance fit is also insufficient due to the five different Mo–O distances in the MoO_3 first shell.

In both types of tests all calculated coordination numbers, with the exception of MoO_3, were within ±30% of the correct value with most values better than ±20%. Debye–Waller correction did not always increase the accuracy of the calculation.

Oxide Catalysts

Several oxide $CoMo/\gamma\text{-}Al_2O_3$ catalysts were examined with EXAFS at the Mo *K* absorption edge. These included catalysts obtained from American Cyanamid (HDS-2A), U.O.P., and Alpha Ventron. Also included was an American Cyanamid $NiMo/\gamma\text{-}Al_2O_3$ (HDS-3A). Only the results from the American Cyanamid HDS-2A are presented here. In Fig. 5 a large peak at about 1.4 Å may be attributed to the Mo–O coordination with a calculated distance of 1.73 Å. Recall that the peak position on the radial structure function is downshifted from the true distance by about 0.4 Å. A smaller peak appears at about 2.1 Å which if attributed to Mo–O would yield a bond length of 2.40 Å. All oxide catalysts examined exhibited similar characteristics. All had essentially the same first-peak magnitude and all

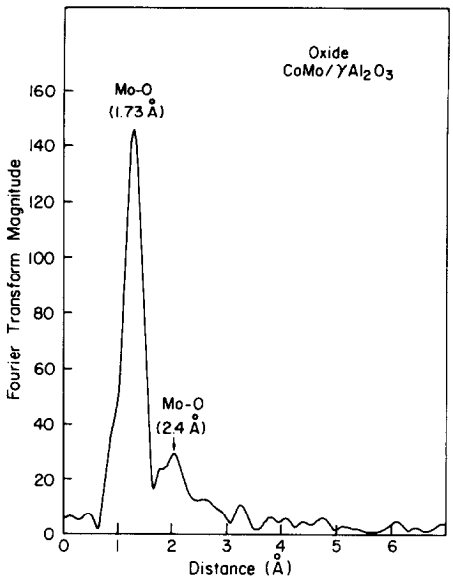

FIG. 5. Fourier transform for oxide $CoMo/\gamma\text{-}Al_2O_3$.

had some evidence of a second peak at about 2.40 Å. The 2.4-Å peak probably represents longer Mo–O bonds in the first Mo coordination shell. However, the possibility cannot be ruled out that this broad peak also contains contributions from short Mo–Al distances. A distance of 2.4 Å is close to the Mo–S distance in MoS_2 but this peak was always present in catalyst samples that had never been exposed to sulfur in any form.

None of the oxide catalysts examined show any evidence of a second shell of atoms. The oxide catalyst in Fig. 5 can be compared to MoO_3 in Fig. 2 or to $\alpha\text{-}CoMoO_4$ in Fig. 3, both of which have large peaks appearing at about 3.1 Å due to the Mo–Mo and Mo–Co backscattering in their second shell of neighbors. The absence of the first-shell triplet rules out $\alpha\text{-}CoMoO_4$ as the major surface species while the average Mo–O bond length of 1.73 Å is far too short to be caused by crystalline MoO_3. The lack of a second shell suggests either a large degree of disorder or very small crystallites. However, the $Na_2MoO_4 \cdot 2H_2O$ presented in Fig. 1 shows only a small second shell at about 3.2 Å due to the low backscattering of Na, H, and O and the relatively long dis-

tance between Mo atoms in the crystal. The possibility that Mo on the oxide catalyst is incorporated into a crystalline compound with the alumina substrate cannot be ruled out on the basis of these EXAFS experiments.

Most recent studies of this catalyst system suggests that Mo is present as Mo(+6) and is four or six coordinated, depending on loading and preparation technique (*1, 2, 33–36*). Coordination calculations based on the curve-fitting techniques described earlier yield Mo–O coordination numbers somewhat lower than expected. The total Mo–O coordination is calculated to be about four oxygens around the molybdenum. The first peak at 1.73 Å contributes a coordination number of 2.5 and the second peak has a coordination number of about 1.2. EXAFS measurements were studied at both 77 and 300°K with similar results for the coordination at both temperatures. It is probable that this calculated coordination number of less than 4 should not be taken seriously since there may be a considerable amount of non-Gaussian disorder and/or multiple-bond distances occurring in the first-coordination shell. Additional modeling based on the results from angle-resolved measurements on single crystals of model compounds and on XANES will be reported subsequently.

An alternative interpretation has been suggested by Chiu and Bauer (*37*) based on area measurements. Their technique compares the area and peak broadening to model compounds with varying degrees of first-shell distortion. This approach has yielded coordination numbers between 4 and 6.

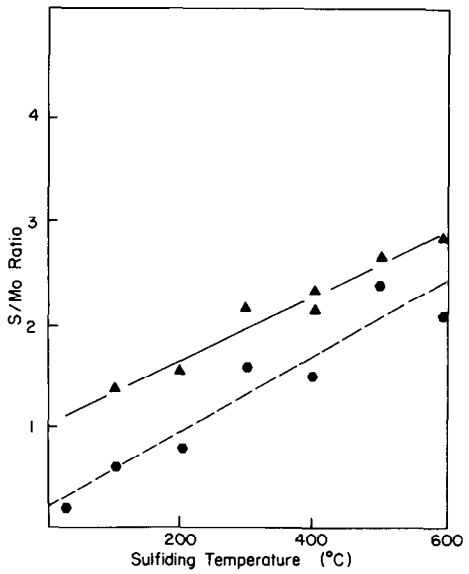

FIG. 6. S/Mo ratio calculated from total sulfur content (▲) and S/Mo calculated from EXAFS coordination numbers (●) plotted vs sulfiding temperatures.

Sulfide Catalysts

Samples of American Cyanamid HDS-2A were sulfided at temperatures from 25 to 600°C in 1 : 9 $H_2S : H_2$. The sulfur content of these specimens was measured by a high temperature pyrolysis procedure by K. Heiden and R. Johnson of Universal Oil Products.

It is necessary to assume a reaction path and thus a stoichiometry to calculate the S/Mo ratio from total sulfur measurements. No information was available on the degree of Co sulfiding, so a conservative assumption was made that all CoO was sulfided entirely to Co_9S_8 at all temperatures. The reaction used for Mo was

$$MoO_3 + 2H_2S + S_2 \rightarrow MoS_2 + 3H_2O$$

The calculated S/Mo ratio vs sulfiding temperature is presented in Fig. 6. The values obtained are well in excess of the bulk MoS_2 ratio of 2 for all sulfiding temperatures above 300°C, and are in reasonable agreement with similar measurements reported elsewhere (*13*) for the sulfiding procedures used in this work.

The radial structure functions for three of the seven sulfiding temperatures are presented in Fig. 7–9. The structural changes in the catalyst with increasing sulfiding temperature are readily apparent in these figures. Figure 7 presents a catalyst sulfided at 100°C. Two major peaks are present. The first peak at about 1.4 Å is the 1.73-Å Mo–O bond that was present on the oxide cata-

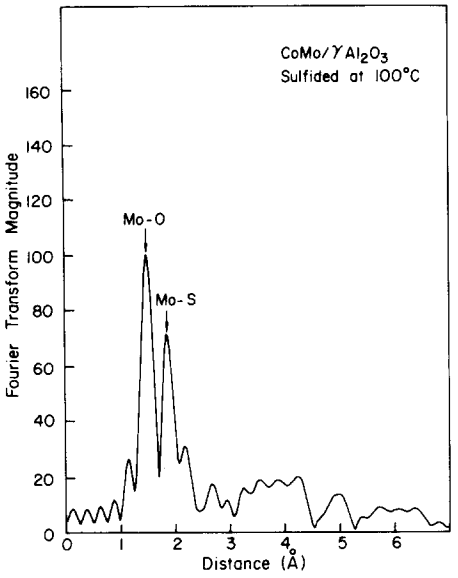

FIG. 7. Fourier transform for CoMo/γ-Al_2O_3 catalyst sulfided at 100°C for 4 h in 1 : 9 H_2S : H_2.

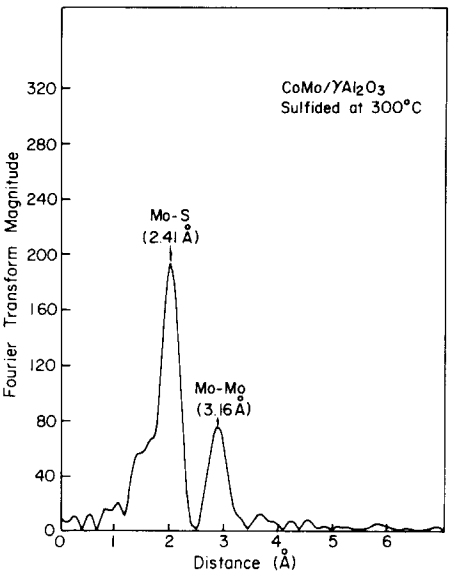

FIG. 8. Fourier transform for CoMo/γ-Al_2O_3 catalyst sulfided at 300°C for 4 h in 1 : 9 H_2S : H_2.

lyst in Fig. 5. The second peak at about 1.8 Å may be attributed to a Mo–S bond that was not present on the oxide catalyst. EXAFS provides an average radial structure function so it is not possible to determine if all Mo atoms are surrounded by both oxygen and sulfur atoms or if some are surrounded by oxygen and some by sulfur. It is important to notice that no second shell is apparent in this figure, implying that the sulfur is not associated with a well-ordered MoS_2 crystallite.

A catalyst sulfided at 300°C is presented in Fig. 8. In this figure there are also two major peaks, but they are quite different from the 100°C sulfided catalyst. The first peak is at about 1.9 Å and represents a Mo–S bond of 2.41 Å. The Mo–O peak that was present on the oxide catalyst is reduced in height and masked by the side of this Mo–S peak. On this sulfide catalyst a discrete second-shell peak is present at about 2.9 Å. Both the Mo–S distance and the Mo–Mo distance on this 300°C sulfided catalyst are in agreement with the interatomic distances for crystalline MoS_2. This figure may be compared to the radial structure function for MoS_2 in Fig. 4. An obvious difference is that relative magnitudes of the Mo–Mo peaks. The Mo–Mo peak on the sulfided catalyst is much smaller relative to the Mo–S peak which implies either a lower coordination number or configurational disorder in the second shell. Small crystallites (<30 Å) of MoS_2 on the catalyst surface would

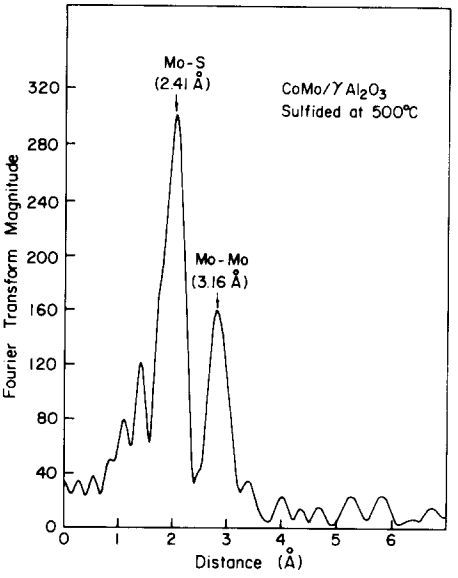

FIG. 9. Fourier transform for CoMo/γ-Al_2O_3 catalyst sulfided at 500°C for 4 h in 1 : 9 H_2S : H_2.

readily explain this effect, as would a chain-like structure. Figure 9 presents the radial structure function for a catalyst specimen sulfided at 500°C. The structure of this catalyst is similar to the 300°C sulfided catalyst except the magnitudes of both the Mo–S peak at about 1.9 Å (2.41 Å actual) and the Mo–Mo peak at about 2.9 Å (3.16 Å actual) are increased.

Quantitative coordination number and distance calculations were made using MoS_2 for the model compound for the Mo–S and Mo–Mo distances. The calculated values are included in Table 5. The coordinations were calculated both with and without Debye–Waller correction. As has been mentioned above, Debye–Waller correction may be inappropriate if non-Gaussian disorder is present.

The uncorrected coordination values for Mo–S and Mo–Mo vs sulfiding temperature are presented in Fig. 10. When sulfiding was done at 25°C essentially no sulfur was coordinated with Mo even though the chemical analysis shows a S/Mo ratio of 1. It can be seen from Fig. 10 that the average sulfur coordination increased rather linearly as the sulfiding temperature was increased. Neither the Mo–S nor the Mo–Mo coordination numbers reached the bulk values of 6.

In Fig. 9, the 500°C sulfided catalyst, no evidence is seen for either the 3.98-Å Mo–S or the 5.46- and 6.32-Å Mo–Mo peaks that

TABLE 5

Mo–S and Mo–Mo Coordination Number Calculations

Sulfiding temperature (°C)	Mo–S		Mo–Mo	
	N	$N\sigma$	N	$N\sigma$
25	0.2	0.2	—	—
100	0.6	0.5	—	—
200	0.9	1.0	0.2	0.6
300	2.2	2.9	0.9	1.6
400	2.4	2.7	1.3	1.7
500	3.7	4.6	1.9	3.1
600	3.8	3.2	2.6	3.8

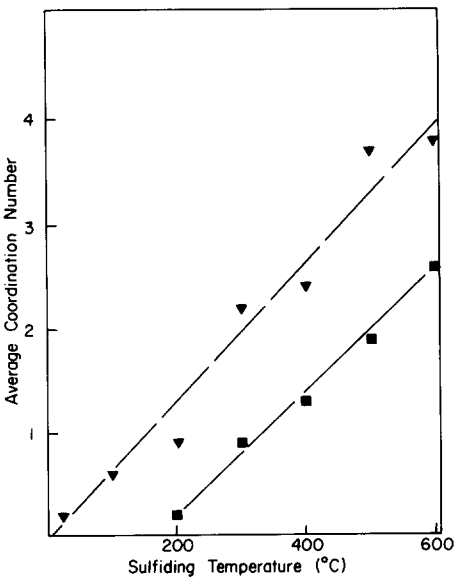

FIG. 10. Coordination numbers calculated from EXAFS for sulfided $CoMo/\gamma\text{-}Al_2O_3$ catalysts. Mo–S (▲) and Mo–Mo (■) plotted vs sulfiding temperature.

are observed in crystalline MoS_2. On the 600°C sulfided catalyst the multiple-scattered 6.32-Å shell is barely observable. Recent studies done *in situ* with measurements at 77°K provide more substantial evidence that the Mo is indeed small crystallites of MoS_2. Exceptionally good quality spectra were obtained to 17.8 $Å^{-1}$ in k-space, providing excellent resolution. The interference function and radial structure function for a catalyst sulfided *in situ* at 400°C is compared to a similar spectra of MoS_2 in Fig. 11. The second Mo–S shell is apparent as are both the second and third Mo–Mo shells at 5.46 and 6.32 Å. Crystalline MoS_2 has been reported earlier on high temperature sulfided catalysts by Pollack *et al.* (*4*) who reported crystallite sizes on the order of 90–140 Å in the basal plane.

Various workers have commented on the sensitivity of the catalyst to air contact. Two of the sulfided catalysts (250 and 400°C sulfiding) were exposed to air and then their EXAFS spectra were measured. No change was observed in the catalyst structure during the first 30 min of air exposure at 25°C. Thus the glovebag handling procedures

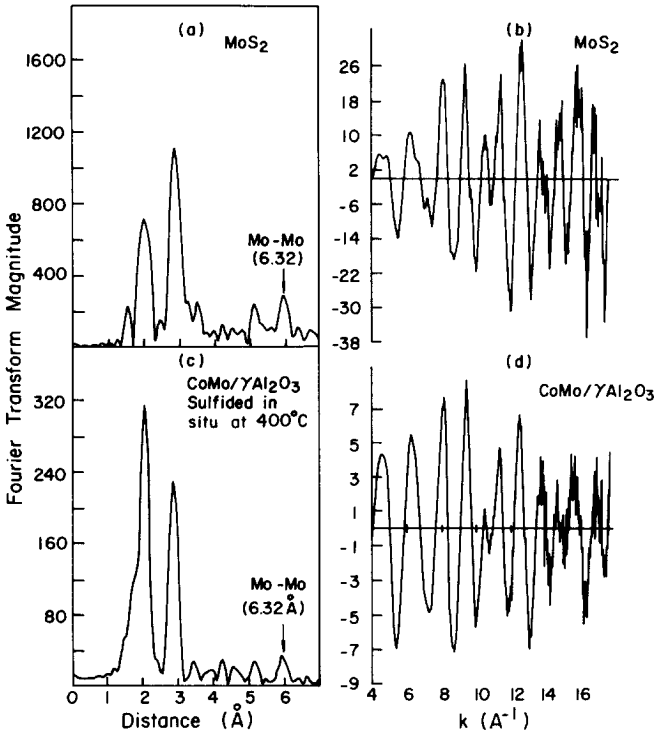

FIG. 11. Interference functions and radial structure functions for MoS_2 and CoMo/γ-Al_2O_3 catalyst sulfided *in situ* at 400°C. Both spectra were measured at 77°K and were transformed over the range k = 3.7–17.7 Å^{-1}. The 6.32-Å multiple-scattered Mo–Mo peak is observed on the sulfided catalyst.

used here seem to be adequate. Both specimens showed about a 20% reduction in Mo–S coordination after overnight exposure to room temperature air. Some increase in the Mo–O coordination was obvious, whereas little change was observed in the Mo–Mo peak at 3.16 Å, suggesting an isomorphic substitution into the MoS_2-like structure.

Two specimens were prepared to test for observable structure modifications due to reduction of the oxide catalyst and prereduction of the catalyst prior to sulfiding. Figure 12 shows the Fourier transform for a specimen reduced in hydrogen at 400°C for 2 h. A slight reduction of the Mo–O peak height was accompanied by the appearance of a peak at 2.4 Å which represents the first Mo–Mo distance for crystalline BCC Mo (2.73 Å). While most of the Mo on the catalyst surface was not reduced, some was apparently reduced to metallic Mo. Note that

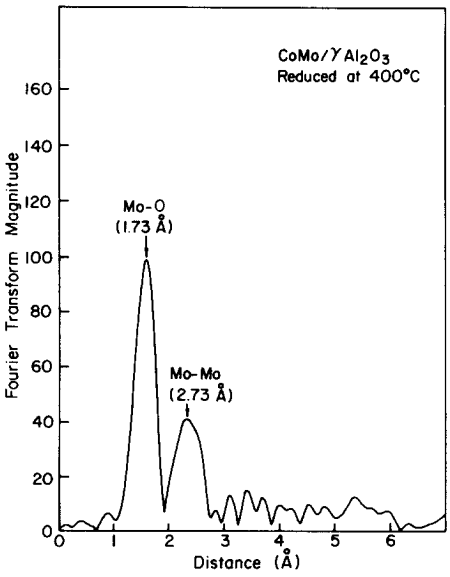

FIG. 12. Fourier transform for CoMo/γ-Al_2O_3 catalyst reduced at 400°C for 4 h in H_2.

only the portion of Mo with adjacent Mo neighbors will contribute to this 2.73-Å peak and thus be observed in the EXAFS spectra, implying migration and aggregation of Mo atoms to form at least Mo dimers with separations close to those in bulk Mo metal. The magnitude of the 2.73-Å Mo–Mo peak is very small compared to that in bulk Mo metal implying that only a small portion of Mo was reduced to zero valent Mo.

A sample of oxide catalyst was prereduced for 2 h at 400°C in hydrogen and then sulfided at 400°C for 4 h. No significant structural difference of this material compared to that sulfided in the usual manner at 400°C was detectable with our EXAFS measurement. No significant change in total measured sulfur was observable.

DISCUSSION AND CONCLUSIONS

The EXAFS measurements yield a calculated Mo–O coordination on oxide CoMo/γ-Al_2O_3 of approximately 3–4. Other techniques have suggested values between 4 and 6. Though disorder could account for the low values we are continuing our work on the oxide form of the catalyst. A subsequent paper will report that work in detail. The absence of a second-coordination shell peak for the oxide catalysts examined indicates that the oxide is well dispersed. This study demonstrates clearly that the Mo is present as neither MoO_3 or α-$CoMoO_4$ in their crystalline forms. Kohatsu *et al.* (*5*) reported a coordination number of 4 at 1.73 Å and 2 at 2.35 Å. Our results qualitatively agree in that a large Mo–O peak was observed at 1.73 Å and a small peak that may be attributed to a Mo–O distance of 2.40 Å. However, we were unable to find any quantitative support for a coordination number of 4 in the first Mo–O distance. Data presented by Topsøe show only the large peak at about 1.73 Å (*6*).

These results all suggest that the molybdenum on the oxide catalyst is present in a well-dispersed oxide phase with the oxide ligands in an unsymmetrical coordination. The apparent average of the several Mo–O distances is significantly smaller than that in MoO_3, in fact within 0.03 Å of the tetrahedral molybdate. This should not be construed to mean that tetrahedral molybdates are the dominant surface species, only that the average of the oxide ligands is at 1.73 Å.

Catalysts sulfided at 100°C and below do not form MoS_2. Rather a Mo–S distance is observed that appears to be somewhat longer (2.47 Å) than in bulk MoS_2 (2.41 Å). This longer Mo–S bond suggests that sulfiding may initially involve formation of Mo–S–H or polysulfide moieties. No Mo–Mo shell is observed under such mild sulfiding conditions. These results suggest that initial sulfur uptake might involve substitution of Mo–S–H for terminal oxygens with little structural effect on the disperse oxide catalyst. At higher sulfiding temperatures (200°C and above) Mo–Mo scatterings are observed in the EXAFS, implying sufficient structural rearrangements have occurred to form small MoS_2 crystallites. The size of the crystallites increases with increased sulfiding temperature.

It is possible to estimate the amount of sulfur coordinated with Mo from our EXAFS results. To do so it was assumed that all sulfided Mo atoms were six-coordinated with sulfur. This assumption obviously is less valid for lightly sulfided catalysts than for the high temperature sulfiding treatments where most of the Mo is sulfided. The portion of Mo that is sulfided, X_{ms}, is then found from the observed Mo–S coordination in the sulfided, X_{ms}, is then found from the observed Mo–S coordination in the EXAFS measurement (C_{ms}).

$$X_{ms} = C_{ms}/6 \qquad (4)$$

Within a MoS_2 crystallite, the S/Mo ratio is a simple function of the Mo–Mo coordination. For an infinite crystal, S/Mo is 2. For a "crystal" with only one Mo atom, the S/Mo ratio is 6. It can be shown that

$$S/Mo = 6 - 2/3\ C_{mm} \qquad (5)$$

This S/Mo ratio must of course be cor-

rected since only X_{ms} of the Mo is involved in the MoS_2 crystallites. Thus

$$S/Mo = X_{ms}(6 - 2/3\ (C_{mm}/X_{ms})) \quad (6)$$

$$S/Mo = C_{ms} - 2/3\ C_{mm} \quad (7)$$

This last relationship holds equally well if the sulfided Mo is tied up in one large crystallite with internal defects or in many very small crystallites.

Calculated values of C_{ms} and C_{mm} from Table 5 were used to calculate S/Mo ratios at various temperatures. These are presented in Fig. 6 (▲), where they are compared to S/Mo ratios from the sulfur analysis. They are significantly lower than the values obtained from chemical analysis (●), and are in essential agreement with Massoth and Chung (*3*). The S/Mo ratios from the chemical analysis are, however, in agreement with de Beers *et al.* (*13*). Massoth has suggested that the higher S/Mo level obtained by de Beers *et al.* is "non-stoichiometric" sulfur which is not associated with the Mo. Our results support this interpretation. In fact, subsequent *in situ* work has shown that significant amounts of sulfur can be desorbed from the catalyst by purging with N_2, but this sulfur removal leaves the Mo–S coordination unchanged.

Our findings on sulfided $CoMo/\gamma\text{-}Al_2O_3$ are in agreement with those measured on $NiMo/\gamma\text{-}Al_2O_3$ by Kohatsu *et al.* (*5*). They observed the reduced Mo–Mo coordination and attributed it to an open network of (MoS_6) subunits or isolated clusters rather than edge sharing as in MoS_2. This interpretation appears reasonable for the lower sulfiding temperatures. Our results are in qualitative agreement with Topsøe (*6*) but we do not find that the sulfiding is complete, especially at temperatures below 300°C. At the highest temperatures examined essentially no Mo–O could be detected, but the measured Mo–S coordination still was less than 6. Our study shows a smooth progression from very isolated Mo–S subunits toward larger crystallites of MoS_2. The presence of a multiple-scattering feature at 6.32 Å (the third Mo–Mo shell) confirms the presence of bulk-like MoS_2.

ACKNOWLEDGMENTS

We acknowledge the technical assistance of the CHESS staff, particularly that of D. Mills, and American Cyanamid and Universal Oil Products for providing the catalysts. The measurements of sulfur levels in sulfided catalysts were carried out by Universal Oil Products. X-Ray diffraction measurements were accomplished at the Cornell Materials Science Center. Financial assistance from the John McMullen Fellowship Fund, Cornell Chemical Engineering Department, and the Materials Science Center at Cornell is also gratefully acknowledged.

This work and its interpretation has benefited greatly by discussions with Professor Simon Bauer and Dr. N. S. Chiu at Cornell, Dr. Arthur Sleight at Du Pont, and Professor Frank Massoth at the University of Utah.

REFERENCES

1. Massoth, F. E., "Advances in Catalysis," Vol. 27, p. 265. Academic Press, New York, 1978.
2. Ratnasamy, P., and Sivasanker, S., *Catal. Rev.-Sci. Eng.* **22**(3), 401 (1980).
3. Furimsky, E., *Catal. Rev.-Sci. Eng.* **22,** 371 (1980).
4. Pollack, S. S., Makovsky, L. E., and Brown, F. R., *J. Catal.* **59,** 452 (1979).
5. Kohatsu, I., Blakely, D. W., and Harnsberger, H. F., *in* "Synchrotron Radiation Research," (H. Winick and S. Doniach, Eds.), p. 417. Plenum Press, New York, 1980.
6. Clausen, B. S., Topsøe, H., Candia, R., Villadsen, J., Lengeler, B., Als-Nielson, J., and Christensen, F., *J. Phys. Chem.* **85**(25), 3868 (1981).
7. Clausen, B. S., Lengeler, B., Candia, R., Als-Nielson, J., and Topsøe, H., *Bull. Soc. Chim. Belg.* **90**(12), 1249 (1981).
8. Topsøe, H., "Advances in Catalytic Chemistry II." Salt Lake City, May 18–21, 1982.
9. American Cyanamid sales literature.
10. Massoth, F. E., *J. Catal.* **36,** 164 (1975).
11. Massoth, F. E., and Chung, K. S., *Fuel Proc. Technol.* **2,** 57 (1979).
12. Chung, K. S., and Massoth, F. E., *J. Catal.* **64**(2), 332 (1980).
13. de Beer, V. H. J., Bevelander, C., van Sint Fiet, T. H. M., Werter, P. G. A., and Amberg, C. H., *J. Catal.* **43,** 68 (1976).
14. Parham, T. G., and Merrill, R. P., Amer. Chem. Soc. Annual Meeting. Kansas City, Mo., Sept. 13–15, 1982.
15. Smith, G. W., and Ibers, J. A., *Acta Crystallogr.* **19,** 269 (1965).

16. Sleight, A. W., and Chamberland, B. L., *Inorg. Chem.* **7,** 1672 (1968).
17. Lee, P. A., Citrin, P. H., Eisenberger, P., and Kincaid, B. M., *Rev. Mod. Phys. Part 1* **53**(4) 769 (1981).
18. Citrin, P. H., Eisenberger, P., and Kincaid, B. M., *Phys. Rev. Lett.* **36**(22), 1346 (1976).
19. Cramer, S. P., SSRL Report 78/07, June 1978.
20. Cramer, S. P., Hodgson, K. O., Stiefel, E. I., and Newton, W. E., *J. Amer. Chem. Soc.* **100**(9), 2748 (1978).
21. Eisenberger, P., and Brown, G. S., *Solid State Commun.* **29,** 481 (1979).
22. Lengeler, B., and Eisenberger, P., *Phys. Rev. B* **21**(10), 4507 (1980).
23. Atovmyan, L. O., and Yackenko, O.A.D., *J. Struct. Chem. (Zh. Strukt. Khim.)* **10,** 504 (1969).
24. Matsumoto, K., Kobayashi, A., and Sasaki, Y., *Bull. Chem. Soc. Jpn.* **48**(3), 1009 (1975).
25. Mitra, R. P., and Verma, H. K. L., *Indian J. Chem.* **7,** 598 (1969).
26. Kihlborg, L., *Ark. Kemi* **21**(34), 357 (1963).
27. Dickinson, R. G., and Pauling L., *J. Amer. Chem. Soc.* **45,** 1466 (1923).
28. To be submitted for publication.
29. Lee, P. A., and Pendry, J. B., *Phys. Rev. B* **11**(8), 2795 (1975).
30. Lee, P. A., and Beni, G., *Phys. Rev. B* **15**(6), 2862 (1977).
31. Teo, B. K., and Lee, P. A., *J. Amer. Chem. Soc.* **101,** 2815 (1979).
32. Gatehouse, B. M., and Leverett, P., *J. Chem. Soc. (A), Inorg. Phys. Theor.* **5,** 849 (1969).
33. Lipsch, J. M. J. G., and Schuit, G. C. A., *J. Catal.* **15,** 174 (1969).
34. Fransen, T., van der Meer, O., and Mars, P., *J. Catal.* **42,** 79 (1976).
35. Walton, R. A., *J. Catal.* **44,** 335 (1976).
36. Medema, J., van Stam, C., de Beer, V. H. J., Konings, A. J. A., Koningsberger, D. C., *J. Catal.* **53,** 386 (1978).
37. Chiu, N., and Bauer, S., personal communication.